

microRNA-485 inhibits the malignant behaviors of retinoblastoma by directly targeting Wnt3a

XUEMAN LYU, LING WANG, JIA LU, HONG ZHANG and LINA WANG

Department of Ophthalmology, China-Japan Union Hospital of Jilin University, Changchun, Jilin 130033, P.R. China

Received December 11, 2018; Accepted February 15, 2019

DOI: 10.3892/or.2019.7061

Abstract. Deregulation of microRNAs (miRNAs) has been widely reported in retinoblastoma (RB), and the aberrantly expressed miRNAs may serve as crucial epigenetic regulators in the occurrence and development of RB. Therefore, the identification of dysregulated miRNAs in RB may be useful for the development of effective targets for the therapy patients with this disease. miRNA (miR)-485-5p (miR-485) is deregulated in multiple human cancer types and serves crucial roles in their progression and development. However, the expression pattern of miR-485 and its role in RB have not been well investigated. In the present study, expression levels of miR-485 in RB tissues and cell lines were measured using reverse transcription-quantitative polymerase chain reaction (RT-qPCR). The effects of miR-485 overexpression on RB cell proliferation, apoptosis, migration and invasion were examined using Cell Counting Kit-8 assay, flow cytometric analysis and *in vitro* migration and invasion assays, respectively. Xenograft tumor formation assay was utilized to determine the influence of miR-485 on RB tumor growth *in vivo*. The mechanism responsible for the tumor-suppressing roles of miR-485 in RB progression was determined through a series of experiments, including bioinformatics prediction, luciferase reporter assay, RT-qPCR, western blot analysis and rescue experiments. Herein, a marked downregulation of miR-485 expression in human RB tissues and cell lines was observed. miR-485 overexpression suppressed RB cell proliferation, induced cell apoptosis, attenuated cell migration and cell invasion *in vitro*, and restrained the growth of RB cells *in vivo*. Additionally, Wnt3a was revealed to be a direct target gene of miR-485 in RB cells. Wnt3a was upregulated in human RB tissues, and its upregulation was inversely associated with miR-485. Furthermore, the tumor suppressive roles of Wnt3a silencing were similar to those of miR-485 overexpression in RB cells. In addition, restoration of Wnt3a expression partially reversed

the tumor suppressor action of miR-485 in RB cells. However, miR-485 upregulation directly targeted Wnt3a to inhibit activation of the Wnt/ β -catenin signaling pathway in RB cells both *in vitro* and *in vivo*. Notably, these results demonstrated that the tumor-suppressive roles of miR-485 were at least partially mediated by Wnt3a in RB cells. Therefore, miR-485 is a potential therapeutic target for treating patients with RB.

Introduction

Retinoblastoma (RB) is a common childhood cancer that arises from the primitive retinal layer (1). RB accounts for ~2-4% of all childhood malignant tumors with an estimated incidence rate of ~1:15,000-1:20,000 per year in children <5 years old (2). In China, the morbidity and mortality rates of RB have gradually increased in recent years (3). Over the past decade, the therapeutic approaches for RB patients, such as ophthalmectomy, laser photocoagulation, cryotherapy and chemoradiotherapy, have achieved tremendous advancement (4). However, the clinical outcomes of these techniques remain unsatisfactory owing to diagnosis delay, metastasis and chemoresistance (5-7). Inactivation of the *Rb1* gene has been identified as a crucial risk factor that may be closely associated with RB formation and development; however, the detailed underlying molecular mechanisms remain unclear (8). Thus, studies of the mechanisms participating in RB formation and progression are essential for identifying molecular targeted therapeutic methods and improving prognosis.

In recent years, microRNAs (miRNAs) have drawn increasing attention in cancer research (9). miRNAs are a group of non-coding and small (18-25-nucleotides) RNA molecules involved in regulating gene expression (10). miRNAs are thought to negatively regulate gene expression by directly interacting with miRNA 'seed' regions to complementary sequences in the 3'-untranslated regions (3'-UTR) of their target genes, which triggers mRNA degradation and/or transcription suppression (11). In total, 1,881 precursor and 2,588 mature miRNAs have been validated in humans, and these miRNAs were predicted to modulate ~67% of all human protein coding genes (12). It has been reported that various miRNAs are dysregulated in RB, and changes in the expression of miRNAs are likely involved in RB initiation and progression (13). miRNAs may serve tumor suppressive or oncogenic roles in the pathogenesis of RB, in which oncogenic miRNAs are highly expressed, whereas tumor-suppressing miRNAs are

Correspondence to: Professor Lina Wang, Department of Ophthalmology, China-Japan Union Hospital of Jilin University, 126 Xiantai Road, Changchun, Jilin 130033, P.R. China
E-mail: lina_wang001@126.com

Key words: retinoblastoma, microRNA-485, proliferation, metastasis, apoptosis, Wnt3a

downregulated in RB (14-16). Therefore, RB-specific associated miRNAs are attractive therapeutic targets for treating patients with this malignancy.

miRNA (miR)-485-5p (henceforth called miR-485) has been frequently reported to be deregulated in multiple human cancer types and serves crucial roles in their progression and development (17-21). However, the expression pattern and roles of miR-485 in RB are unclear. In the present study, the aberrant expression and relevant biological roles of miR-485 in RB was investigated. Furthermore, the mechanism responsible for the tumor-suppressing roles of miR-485 in RB progression was determined.

Materials and methods

Patients and tissue specimens. The present study was approved by the Ethics Committee of China-Japan Union Hospital of Jilin University (Changchun, China). Written informed consent was provided by all donors enrolled in this study. A total of 26 human RB tissues were obtained from patients diagnosed with RB (17 males, 9 females; age range, 14-48 years) and subjected to enucleation at the China-Japan Union Hospital of Jilin University between September 2015 and July 2017. Normal retinal tissues as a control group were collected from the globe rupture of seven patients (3 males, 4 females; age range, 35-62 years). No patients had been treated with chemotherapy or radiotherapy prior to surgery. Patients treated with chemotherapy or radiotherapy were excluded from this research. All tissue specimens were immediately frozen in liquid nitrogen after surgical resection and then stored at -80°C.

Cell lines. In total, three human RB cell lines (Y79, SO-RB50 and Weri-RB1) and a normal retinal pigmented epithelial cell line (ARPE-19) were purchased from American Type Culture Collection (Manassas, VA, USA). Dulbecco's modified Eagle's medium (DMEM) supplemented with 10% fetal bovine serum (FBS) and 1% penicillin-streptomycin mixture (all from Gibco; Thermo Fisher Scientific, Inc., Waltham, MA, USA) was used to culture all cell lines. Cells were grown at 37°C in a 95% humidified atmosphere containing 5% CO₂. Y79 and Weri-RB1 cells exhibited relatively lower miR-485 expression levels among the three RB cell lines, and were therefore used in all subsequent experiments.

Transfection assay. Synthetic miR-485 mimics (5'-AGA GGCUGGCCGUGAUGAAUUC-3') and miRNA mimic negative control (miR-NC; 5'-UUCUCCGAACGUGUCACG UTT-3') were obtained from Shanghai GenePharma Co., Ltd. (Shanghai, China). To silence Wnt3a, a small interfering (si) RNA targeting Wnt3a (Wnt3a siRNA; 5'-CCCACUCGGAUA CUUCUATT-3') and a negative control siRNA (NC siRNA; 5'-UUCUCCGAACGUGUCACGUTT-3') were chemically generated by Guangzhou RiboBio Co., Ltd. (Guangzhou, China). For Wnt3a restoration, the expression construct of Wnt3a pCMV-Wnt3a and empty pCMV plasmid were synthesized by the Chinese Academy of Sciences (Changchun, China). The cells were plated into 6-well plates at a density of 5x10⁵ cells/well. When the density reached ~60-70% confluency, cells were transfected with miR-485 mimics

(100 pmol), miR-NC (100 pmol), Wnt3a siRNA (100 pmol), NC siRNA (100 pmol), pCMV-Wnt3a (4 μg) or empty pCMV plasmid (4 μg) using Lipofectamine[®] 2000 (cat. no. 11668019; Invitrogen; Thermo Fisher Scientific, Inc.). All transfection reaction was performed at room temperature. At different times of incubation, transfected cells were harvested and used in functional experiments. Reverse transcription-quantitative polymerase chain reaction (RT-qPCR), flow cytometric analysis and *in vitro* migration and invasion assays were carried out after at 48 h post-transfection. Cell Counting Kit-8 (CCK-8) assay and western blot analysis was conducted after 24 and 72 h post-transfection, respectively.

RNA extraction and RT-qPCR. The expression levels of miR-485 and Wnt3a mRNA were determined by RT-qPCR analysis. TRIzol[®] reagent (cat. no. 15596026; Thermo Fisher Scientific, Inc.) was used for RNA extraction from tissues (100 mg) or cells (1.5x10⁶ cells). The concentration and purity of the total RNA was assessed using a NanoDrop 2000 spectrophotometer (Thermo Fisher Scientific, Inc., Wilmington, DE, USA). To detect miR-485 expression, total RNA was reverse-transcribed into cDNAs using an miScript Reverse Transcription kit (cat. no. 218061; Qiagen GmbH, Hilden, Germany). The temperature protocols for reverse transcription were as follows: 37°C for 60 min and 95°C for 5 min. Subsequently, qPCR was carried out using a miScript SYBR-Green PCR kit (cat. no. 218073; Qiagen GmbH). The thermocycling conditions were as follows: 95°C for 2 min, followed by 40 cycles at 95°C for 10 sec, 55°C for 30 sec and 72°C for 30 sec. To identify Wnt3a mRNA, cDNA was prepared from total RNA using a PrimeScript RT reagent kit (cat. no. RR037A; Takara Bio, Inc., Otsu, Japan). The temperature protocol was as follows: 37°C for 15 min and 85°C for 5 sec. The synthesized cDNA was amplified using a SYBR Premix Ex Taq[™] kit (cat. no. RR420A; Takara Bio, Inc.). The thermocycling conditions were as follows: 5 min at 95°C, followed by 40 cycles of 95°C for 30 sec and 65°C for 45 sec. U6 small nuclear RNA and GAPDH were used as endogenous controls for the normalization of miR-485 and Wnt3a mRNA expression, respectively. The 2^{-ΔΔC_q} method was used to calculate the relative gene expression (22). The primers were designed as follows: miR-485, forward 5'-CCAAGCTTCCACCATTCCTAACAGGAC-3', reverse 5'-CGGGATCCGTAGGTCAGTTACATGCATC-3'; U6, forward 5'-GCTTCG GCAGCACATATACTAAAAT-3', and reverse 5'-CGCTTC ACGAATTTGCGTGTGCAT-3'; Wnt3a, forward 5'-CATCAA GATTGGCATCCAG-3', and reverse 5'-TGCCTTCTGCAC ATGAGCG-3'; and GAPDH, forward 5'-GTCAATGAAGGG GTCGTTGATGG-3', and reverse 5'-TCGTCCCGTAGACAA AATGGTGA-3'.

CCK-8 assay. Aliquots of 100 μl culture medium containing 3x10³ cells were seeded into each well of 96-well plates, 24 h post-transfection. Cells were incubated at 37°C in a humidified atmosphere containing 5% CO₂. CCK-8 assay was conducted to evaluate cellular proliferation at 0, 24, 48 and 72 h following inoculation. At each time point, 10 μl of CCK-8 solution (cat. no. CK04; Dojindo Molecular Technologies, Inc., Kumamoto, Japan) was added into each well followed by incubation at 37°C for another 2 h. The

absorbance was measured at 450 nm wavelength using an ELISA microplate reader (Bio-Rad Laboratories, Inc., Hercules, CA, USA).

Flow cytometric analysis of cell apoptosis. Following transfection for 48 h, the cells (1×10^6 cells) were harvested and washed with ice-cold PBS (Gibco; Thermo Fisher Scientific, Inc.) thrice. Apoptosis was evaluated using an Annexin V-fluorescein isothiocyanate (FITC) Apoptosis Detection kit (cat. no. 640914; BioLegend, Inc., San Diego, CA, USA). Transfected cells were suspended in 100 μ l of binding buffer followed by incubation with 5 μ l Annexin V-FITC and 5 μ l propidium iodide at room temperature for 30 min, in the dark. Finally, transfected cells were analyzed with a flow cytometer (FACScan™; BD Biosciences) and CellQuest™ software version 5.1 (BD Biosciences, San Jose, CA, USA).

In vitro migration and invasion assays. Cell migratory and invasive abilities were detected using Transwell chamber inserts (8-mm pore size) coated without and with Matrigel (cat. no. 354480; BD Biosciences), respectively. Following 48 h incubation, transfected cells suspended in FBS-free DMEM were plated at a density of 5×10^4 cells/well in the upper compartments. The lower compartments were covered with 600 μ l DMEM containing 10% FBS as a nutritional supplement. After 24 h, the non-migratory or non-invasive cells remaining on the upper surface of the membrane were gently removed with a cotton swab. The migrated and invaded cells were fixed with 100% methanol at 37°C for 20 min, stained with 0.05% crystal violet at 37°C for 20 min, washed with PBS and air-dried. Images of the migrated and invaded cells were captured under an inverted light microscope (x200 magnification; Olympus Corporation, Tokyo, Japan). The cells were counted from five randomly chosen fields/insert.

Xenograft tumor formation assay. All experimental procedures involving animals were approved by the Ethics Committee of China-Japan Union Hospital of Jilin University. Cells transfected with miR-485 mimics or miR-NC were collected after 24 h incubation and resuspended in culture medium. A total of 1×10^6 cells was seeded subcutaneously into the flanks female BALB/c nude mice (n=8; weight, 20 g; age, 4 weeks; Chinese Academy of Sciences; Shanghai, China). There were two groups (n=4 mice/group), one injected with miR-NC transfected cells and the other injected with miR-485 mimics transfected cells; every mouse was injected only once. The animals were maintained under specific pathogen-free conditions (25°C; 50% humidity; 10-h light/14-h dark cycle). Tumor growth was detected every 4 days, and the tumor volume was analyzed using the following formula: Tumor volume = (tumor length x tumor width²)/2. Four weeks after the initial injection, all mice were sacrificed and tumor xenografts were excised and weighed.

Bioinformatics prediction. Three different databases, including TargetScan 7.1 (www.targetscan.org), MiRanda (<http://www.microrna.org/microrna/home.do>) and miRDB (www.mirdb.org), were used to search for putative targets of miR-485.

Luciferase reporter assay. The wild-type (wt) and mutant (mut) 3'-UTR fragments of Wnt3a containing the wt and mut miR-485 binding site, respectively, were chemically constructed by Shanghai GenePharma Co., Ltd., and inserted into the pGL3 luciferase reporter vector (Promega Corporation, Madison, WI, USA). The generated luciferase reporter plasmids were named as pGL3-Wnt3a-3'-UTR-wt and pGL3-Wnt3a-3'-UTR-mut. After culture in 24-well plates, miR-485 mimics or miR-NC were transfected into cells along with pGL3-Wnt3a-3'-UTR-wt or pGL3-Wnt3a-3'-UTR-mut using Lipofectamine® 2000, according to the manufacturer's protocol. Transfected cells were harvested after 48 h of incubation, and luciferase activity was determined using a Dual-Luciferase Reporter Assay System (cat. no. E1910; Promega Corporation) and read using an ELISA microplate reader. Firefly luciferase activity was normalized to that of *Renilla* luciferase activity.

Western blot analysis. Total protein was prepared from RB tissue samples (100 mg), normal retinal tissues (100 mg) or cells (1.5×10^6 cells) using Radioimmunoprecipitation Assay lysis buffer (cat. no. P0013B) and protein concentration was quantified with a Bicinchoninic Protein assay kit (cat. no. P0012; both from Beyotime Institute of Biotechnology, Haimen, China). Protein samples (30 μ g) were separated by 10% SDS-PAGE and transferred to polyvinylidene difluoride membranes (EMD Millipore, Billerica, MA, USA). Subsequently, the membranes were blocked with 5% skim milk at room temperature for 2 h and incubated overnight at 4°C with primary antibodies. The primary antibodies used were as follows: Mouse anti-human monoclonal Wnt3a antibody (cat. no. ab81614; 1:1,000; Abcam, Cambridge, UK), mouse anti-human monoclonal β -catenin antibody (cat. no. sc-59737; 1:1,000; Santa Cruz Biotechnology, Inc., Dallas, TX, USA), mouse anti-human monoclonal phosphorylated (p)- β -catenin antibody (cat. no. sc-57534; 1:1,000; Santa Cruz Biotechnology, Inc.), rabbit anti-human monoclonal cyclin D1 antibody (cat. no. ab134175; 1:1,000; Abcam) and mouse anti-human GAPDH antibody (cat. no. ab9484; 1:1,000; Abcam). The membranes were washed three times with Tris-buffered saline containing 0.1% Tween®-20 for 5 min at room temperature each followed by blotting with corresponding horseradish peroxidase-conjugated secondary antibody (cat. no. ab6789 and ab6721; 1:5,000; Abcam) at room temperature for 2 h. Protein bands were visualized with an electrochemiluminescence advanced Western Blotting Substrate (cat. no. 32109; Thermo Fisher Scientific, Inc.). GAPDH was used for normalization, and densitometric analysis was performed using the Quantity One software version 4.62 (Bio-Rad Laboratories, Inc.)

Statistical analysis. Data are reported as the mean \pm standard deviation from at least three independent experiments. Statistical analysis was conducted using the SPSS 20.0 (IBM Corp., Armonk, NY, USA) by paired Student's t-test for comparisons of two groups, and one-way analysis of variance followed by Student-Newman-Keuls post hoc test for comparisons of multiple groups. The correlation between miR-485 and Wnt3a mRNA levels in RB tissues was examined using Spearman's correlation analysis. $P < 0.05$ was considered to indicate a statistically significant difference.

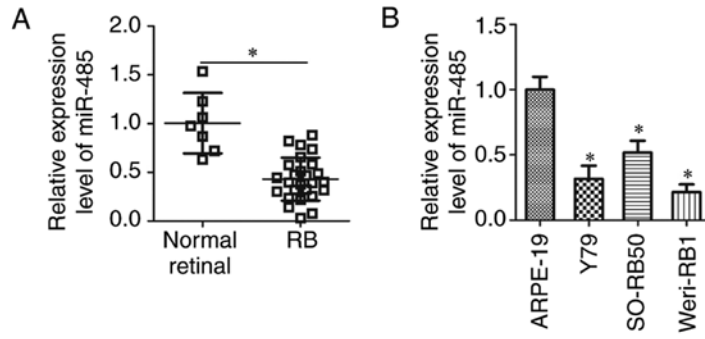


Figure 1. Expression of miR-485 is lower in RB tissues and cell lines. (A) RT-qPCR was performed to examine miR-485 expression in 26 human RB and 7 normal retinal tissues; $P < 0.05$ (B) Quantitative analysis of miR-485 expression in three human RB cell lines (Y79, SO-RB50 and Weri-RB1) and a normal retinal pigmented epithelial cell line (ARPE-19) was conducted through RT-qPCR. * $P < 0.05$ vs. ARPE-19. miR, microRNA; RB, retinoblastoma; RT-qPCR, reverse transcription-quantitative polymerase chain reaction.

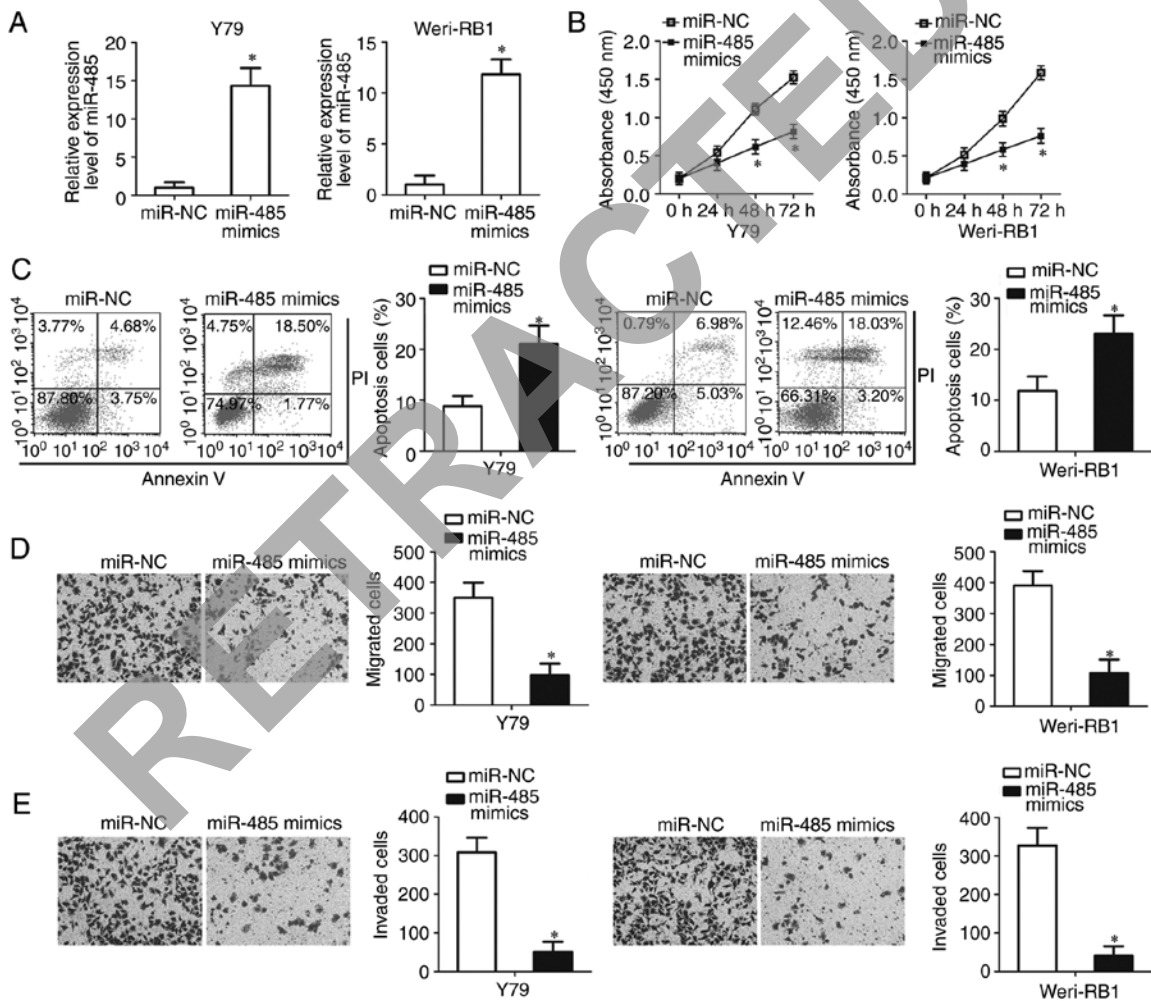


Figure 2. miR-485 serves antitumor roles in the proliferation, apoptosis, migration and invasion of RB cells. (A) The expression of miR-485 in Y79 and Weri-RB1 cells after miR-485 mimics or miR-NC transfection was detected through reverse transcription-quantitative polymerase chain reaction. (B) The proliferation activity of Y79 and Weri-RB1 cells transfected with miR-485 mimics or miR-NC was determined via Cell Counting Kit-8 assay. (C) Flow cytometric analysis was used to measure the percentage of apoptotic Y79 and Weri-RB1 cells that were treated with miR-485 mimics or miR-NC. (D) Migration and (E) invasion of Y79 and Weri-RB1 cells after transfection with miR-485 mimics or miR-NC was evaluated using migration and invasion assays, respectively. * $P < 0.05$ vs. miR-NC. miR, microRNA; NC, negative control; RB, retinoblastoma.

Results

miR-485 expression is downregulated in human RB tissues and cell lines. RT-qPCR was used to detect miR-485

expression levels in 26 human RB and 7 normal retinal tissues. The results demonstrated that the expression levels of miR-485 were significantly lower in RB compared with normal retinal tissues ($P < 0.05$; Fig. 1A). Additionally, miR-485 expression in

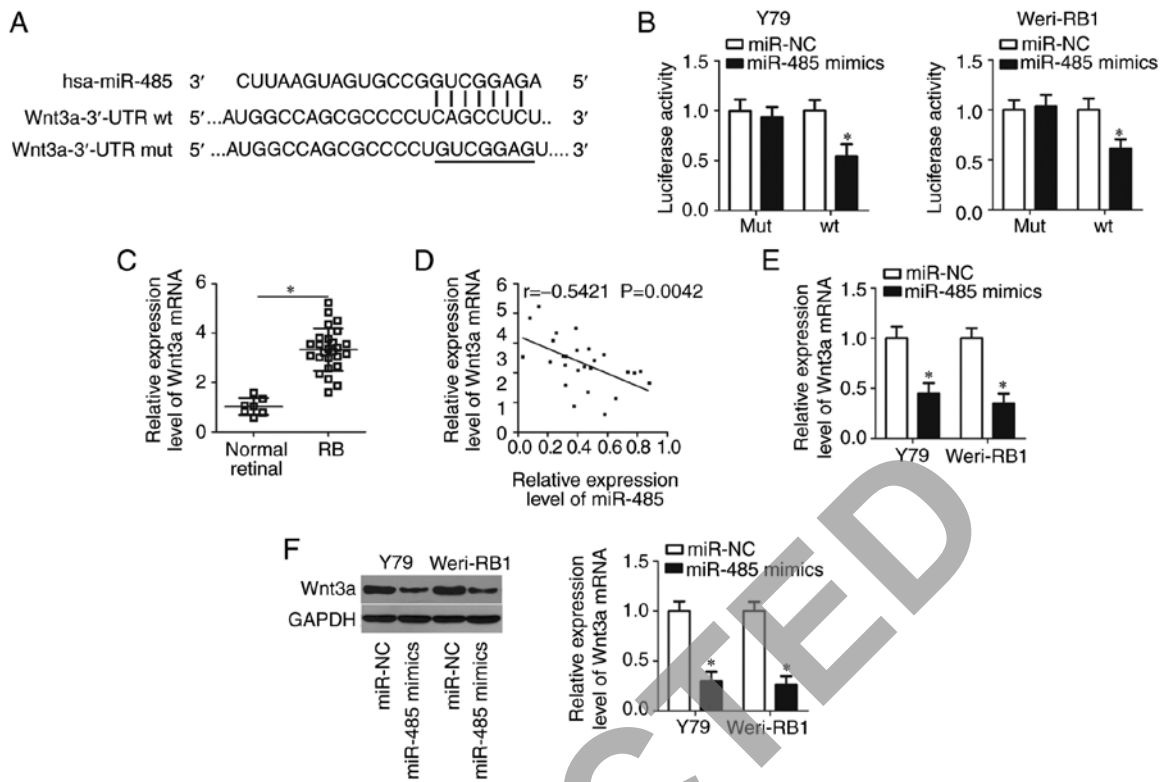


Figure 3. Wnt3a is the target of miR-485 in RB cells. (A) The putative wt and mut miR-485-binding site in the 3'-UTR of Wnt3a gene are shown. (B) Luciferase reporter assay was carried out 48 h after co-transfection in Y79 and Weri-RB1 cells with pGL3-Wnt3a-3'-UTR wt and pGL3-Wnt3a-3'-UTR mut along with miR-485 mimics or miR-NC; * $P < 0.05$ vs. miR-NC. (C) The mRNA expression levels of Wnt3a in 26 human RB tissues and 7 normal retinal tissues was measured through RT-qPCR; * $P < 0.05$ vs. normal retinal tissues. (D) Correlation between miR-485 and Wnt3a mRNA expression in RB tissues was assessed using Spearman's correlation analysis; $r = -0.5421$, $P = 0.0042$. (E) mRNA and (F) protein expression levels of Wnt3a in miR-485 mimics or miR-NC transfected Y79 and Weri-RB1 cells were detected by RT-qPCR and western blot analysis, respectively; * $P < 0.05$ vs. miR-NC. miR-NC, miR, microRNA; mut, mutated; NC, negative control; RB, retinoblastoma; RT-qPCR, reverse transcription-quantitative polymerase chain reaction; wt, wild-type.

three human RB cell lines (Y79, SO-RB50 and Weri-RB1) and a normal retinal pigmented epithelial cell line (ARPE-19) were measured. miR-485 expression levels were significantly lower in all three RB cell lines compared with that in ARPE-19 cells ($P < 0.05$; Fig. 1B). These results demonstrated that miR-485 was decreased in RB tissues and cell lines, which suggested that miR-485 may be involved in RB development.

miR-485 inhibits proliferation, promotes apoptosis and restricts migration and invasion of RB cells. To clarify the roles of miR-485 in RB, miR-485 expression was increased by transfecting Y79 and Weri-RB1 cells with miR-485 mimics ($P < 0.05$; Fig. 2A); these cell lines were selected as they exhibited lower miR-485 expression among the three RB cell lines. The proliferative ability of Y79 and Weri-RB1 cells was examined by CCK-8 assay, which demonstrated a significantly reduced proliferation in cells transfected with miR-485 mimics compared with the miR-NC group ($P < 0.05$; Fig. 2B). Additionally, ectopic miR-485 expression increased the apoptotic rate (early + late) of Y79 and Weri-RB1 cells compared with that in the miR-NC groups ($P < 0.05$; Fig. 2C). Furthermore, the effects of miR-485 overexpression on the migratory and invasive capacities of RB cells was explored using *in vitro* migration and invasion assays. The results demonstrated that increased miR-485 expression significantly decreased the migration ($P < 0.05$; Fig. 2D) and invasion ($P < 0.05$; Fig. 2E) of Y79 and Weri-RB1 cells. Overall, these results indicated that

miR-485 may serve tumor suppressive roles in the development and progression of RB.

Wnt3a is a direct target gene of miR-485 in RB cells. It has been well-documented that miRNAs target the 3'-UTR of their target genes to perform crucial roles in carcinogenesis and cancer progression (23-25). To determine the fundamental mechanisms underlying the action of miR-485, bioinformatics analysis was conducted to search for the potential targets of miR-485. A putative binding site for miR-485 was predicted in the nucleotide sequence from 1,626 to 16,32 of the Wnt3a 3'-UTR (Fig. 3A). Wnt3a was selected for further analysis because this gene is known to serve important roles in tumorigenesis and tumor development (26-28). To explore whether miR-485 directly binds to the 3'-UTR of Wnt3a, luciferase reporter assays were conducted. The data indicated that the luciferase activity of the plasmid carrying the wt miR-485 binding site was decreased by miR-485 overexpression in Y79 and Weri-RB1 cells, but luciferase activity was unaffected in cells transfected with the plasmid carrying the mut miR-485 binding site ($P < 0.05$; Fig. 3B).

Wnt3a expression was detected in RB tissues and its association with miR-485 was further determined. RT-qPCR analysis demonstrated that Wnt3a expression was upregulated in RB compared with the normal retinal tissues ($P < 0.05$; Fig. 3C). Notably, Wnt3a mRNA expression levels were determined to be inversely correlated with that of miR-485 expression

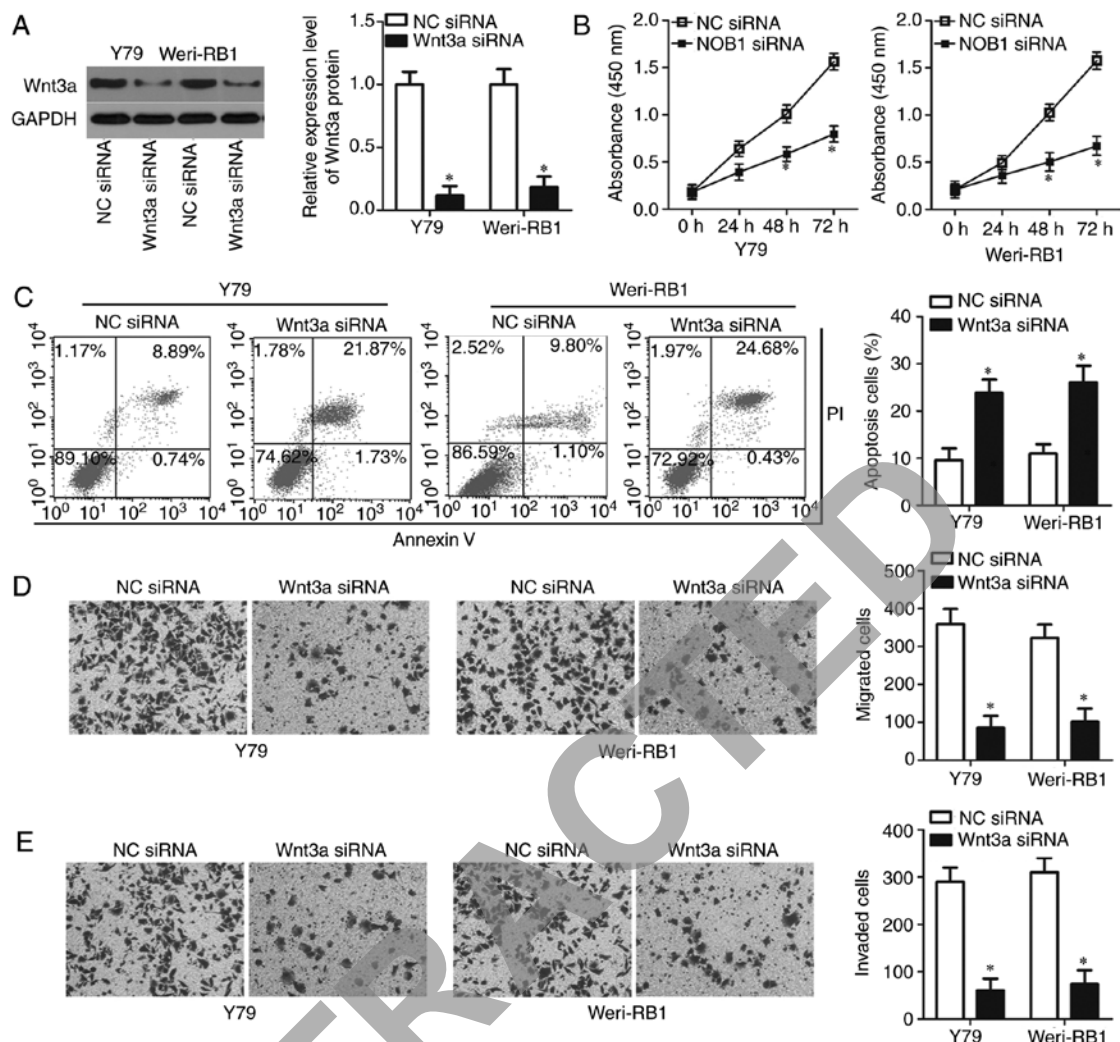


Figure 4. Wnt3a silencing inhibits RB cell proliferation, migration and invasion, inducing cell apoptosis *in vitro*. Wnt3a siRNA or NC siRNA was transfected into Y79 and Weri-RB1 cells. Transfected cells were used in the following assays. (A) Western blot analysis was used to quantify Wnt3a protein expression. (B) Cell Counting Kit-8 assay of the proliferation of the abovementioned cells. (C) The apoptosis rate of aforementioned cells was detected using flow cytometric analysis. (D) Cellular migratory and (E) invasive abilities were analyzed by migration and invasion assays. * $P < 0.05$ vs. NC siRNA. NC, negative control; RB, retinoblastoma; siRNA, small interfering RNA.

in RB tissues ($r = -0.5421$, $P = 0.0042$; Fig. 3D). Furthermore, the expression levels of Wnt3a mRNA ($P < 0.05$; Fig. 3E) and protein ($P < 0.05$; Fig. 3F) were significantly downregulated by miR-485 mimics in Y79 and Weri-RB1 cells, as demonstrated by RT-qPCR and western blot analysis. Taken together, these results demonstrated that Wnt3a is a direct target gene of miR-485 in RB cells.

Wnt3a silencing simulates the activity of miR-485 overexpression in RB cells. To evaluate whether Wnt3a may be involved in RB progression, Wnt3a siRNA was used to silence Wnt3a expression in Y79 and Weri-RB1 cells, which was confirmed by western blot analysis ($P < 0.05$; Fig. 4A). The CCK-8 assay and flow cytometric analysis demonstrated that Wnt3a knockdown attenuated the proliferation ($P < 0.05$; Fig. 4B) and induced the apoptosis ($P < 0.05$; Fig. 4C) of Y79 and Weri-RB1 cells. Furthermore, the effects of Wnt3a inhibition on the migration and invasion of RB cells was determined. The results of the *in vitro* migration and invasion assays demonstrated that treatment with Wnt3a siRNA decreased the migratory ($P < 0.05$;

Fig. 4D) and invasive ($P < 0.05$; Fig. 4E) abilities of Y79 and Weri-RB1 cells. These results indicated that the biological roles of Wnt3a inhibition in RB cells are similar to those induced by miR-485 upregulation, which suggested that Wnt3a is a downstream target of miR-485 in RB cells.

Wnt3a inhibition is required for miR-485-associated phenotypes in RB cells. As Wnt3a was a direct target of miR-485, a series of rescue experiments were performed to determine whether Wnt3a is essential for the tumor-suppressing roles of miR-485 in RB cells. Firstly, the Wnt3a expression plasmid pCMV-Wnt3a without the 3'-UTR or empty pCMV plasmid was transfected into Y79 and Weri-RB1 cells. Western blot analysis confirmed that Wnt3a protein was increased in Y79 and Weri-RB1 cells following pCMV-Wnt3a transfection ($P < 0.05$; Fig. 5A). Subsequently, pCMV-Wnt3a was co-transfected into Y79 and Weri-RB1 cells overexpressing miR-485, and the miR-485-induced decrease in Wnt3a protein expression in Y79 and Weri-RB1 cells was recovered by co-transfection with pCMV-Wnt3a ($P < 0.05$; Fig. 5B). Similarly,

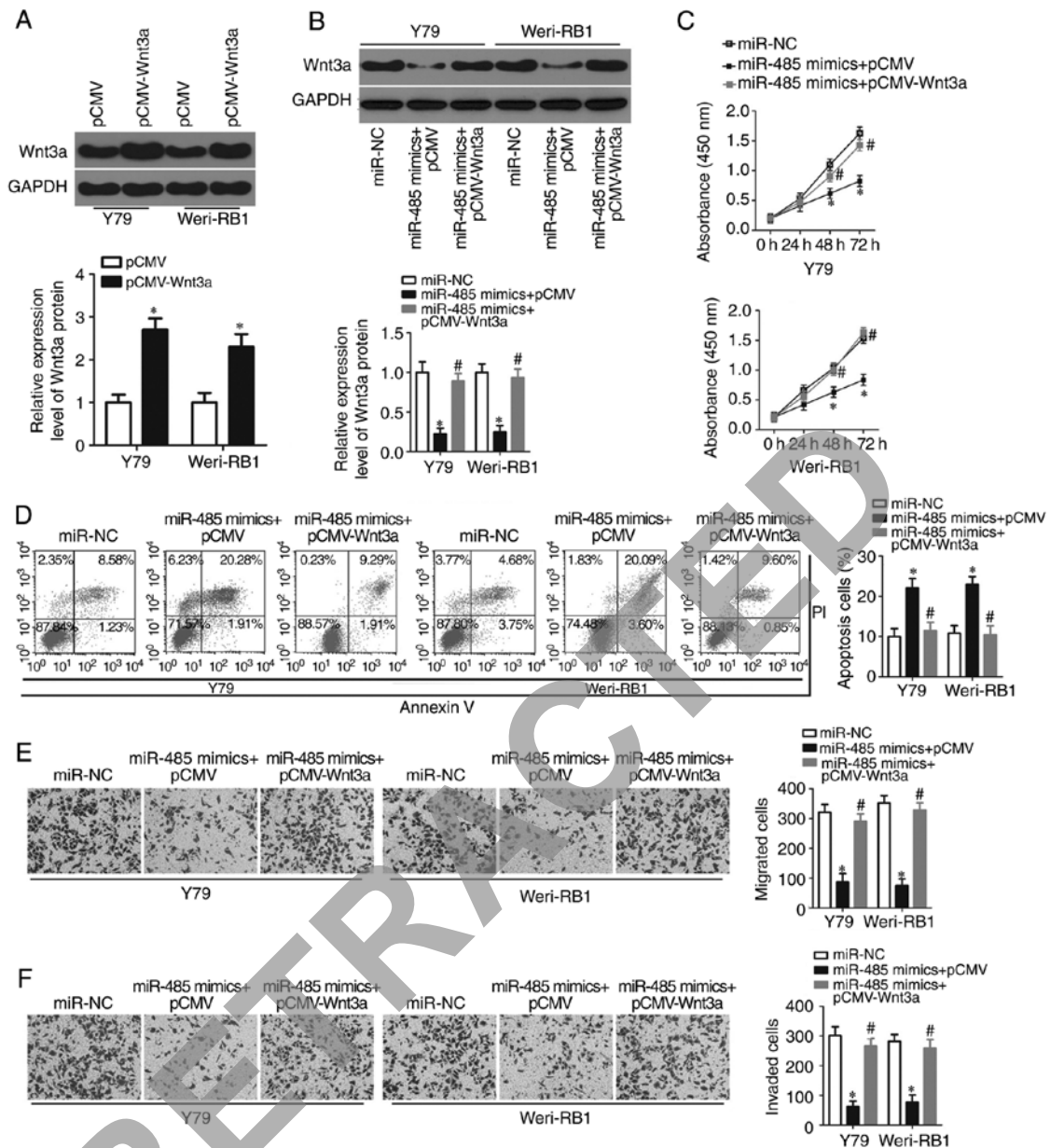


Figure 5. Wnt3a restoration reverses the effects of miR-485 overexpression in RB cells. miR-485 mimics together with Wnt3a expression plasmid pCMV-Wnt3a or pCMV empty plasmid were co-transfected into Y79 and Weri-RB1 cells. (A) Western blot analysis was performed in pCMV-Wnt3a or pCMV-transfected Y79 and Weri-RB1 cells. The results verified that Wnt3a protein expression was upregulated in Y79 and Weri-RB1 cells after transfection with pCMV-Wnt3a; *P<0.05 vs. pCMV. (B) Protein expression of Wnt3a was measured by western blot analysis; *P<0.05 vs. miR-NC; #P<0.05 vs. miR-485 mimics+pCMV. (C) Cell Counting Kit-8 assay, (D) flow cytometric analysis, (E) migration and (F) invasion assays were used to investigate the proliferation, apoptosis, migration and invasion, respectively of Y79 and Weri-RB1 cells treated as above; *P<0.05 vs. miR-NC; #P<0.05 vs. miR-485 mimics+pCMV. miR, microRNA; NC, negative control; RB, retinoblastoma.

functional assays revealed that reintroduction of Wnt3a expression abolished the tumor suppressor activity of miR-485 on RB cell proliferation (P<0.05; Fig. 5C), apoptosis (P<0.05; Fig. 5D), migration (P<0.05; Fig. 5E) and invasion (P<0.05; Fig. 5F). These data further confirmed Wnt3a as a downstream effector of miR-485 in RB cells, and downregulation of Wnt3a is required for the effects of miR-485 on RB cells.

miR-485 inhibits activation of the Wnt/β-catenin signaling pathway in RB cells by directly targeting Wnt3a. Wnt3a is one of the major ligands of the Wnt/β-catenin signaling pathway (26); thus, whether miR-485 is involved in suppressing the Wnt/β-catenin signaling pathway in RB cells through the

regulation of Wnt3a was investigated. Western blot analysis was conducted to detect the expression levels of molecules associated with the Wnt/β-catenin signaling pathway, including p-β-catenin, β-catenin and cyclin D1. The data revealed that miR-485 overexpression decreased the protein expression levels of p-β-catenin and cyclin D1. However, the total level of β-catenin protein expression was unaltered. Additionally, the downregulated p-β-catenin and cyclin D1 protein expression levels caused by miR-485 upregulation were restored in Y79 and Weri-RB1 cells after co-transfection with pCMV-Wnt3a (Fig. 6). These results indicated that miR-485 inhibited the activation of the Wnt/β-catenin signaling pathway in RB cells by directly targeting Wnt3a.

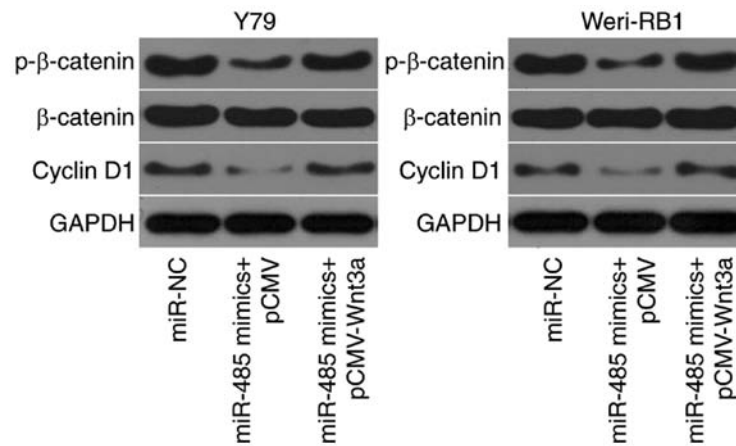


Figure 6. miR-485 overexpression deactivates the Wnt/ β -catenin signaling pathway in RB cells. Y79 and Weri-RB1 cells were co-transfected with miR-485 mimics and pCMV-Wnt3a or pCMV. Following transfection for 72 h, p- β -catenin, β -catenin, and cyclin D1 protein expression levels were determined by western blot analysis. miR, microRNA; NC, negative control; p, phosphorylated; RB, retinoblastoma.

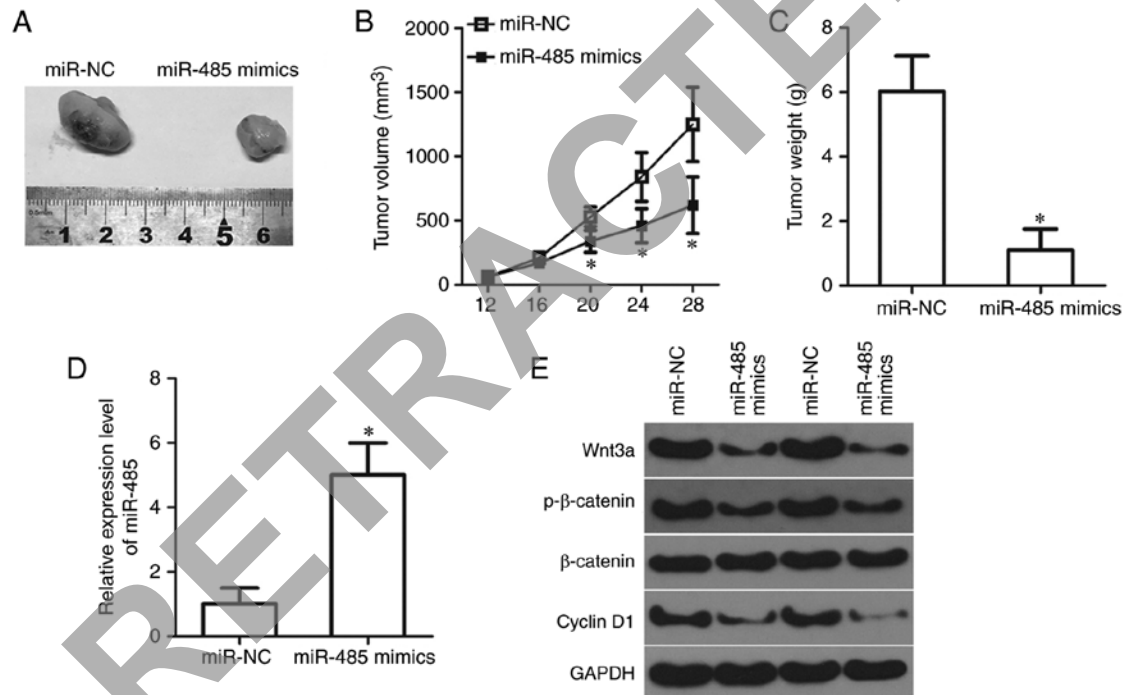


Figure 7. miR-485 hinders tumor growth *in vivo*. (A) Representative images of the tumor xenografts derived from miR-485 mimics or miR-NC groups. (B) Measurement the volume of the tumor xenografts in miR-485 mimics or miR-NC groups. (C) Measurement of the weight of the tumor xenografts. (D) Reverse transcription-quantitative polymerase chain reaction was carried out to detect miR-485 expression in the tumor xenografts. (E) The protein expression levels of Wnt3a, p- β -catenin, β -catenin, and cyclin D1 were quantified by western blot analysis, and the densitometric analysis was performed with Quantity One software version 4.62; * $P < 0.05$ vs. miR-NC. miR, microRNA; NC, negative control; p, phosphorylated; RB, retinoblastoma.

miR-485 inhibits RB growth in vivo. A xenograft tumor formation assay was conducted to further investigate the effects of miR-485 on RB tumor growth *in vivo*. miR-485 mimics or miR-NC-transfected Y79 cells were injected into the flanks of nude mice. The volume of tumor xenografts in nude mice inoculated with miR-485 overexpression-Y79 cells was significantly smaller compared with that in the miR-NC groups ($P < 0.05$; Fig. 7A and B). Tumor growth was also measured for 4 weeks following xenotransplantation. The data revealed that miR-485 upregulation attenuated tumor growth *in vivo* compared with the miR-NC group ($P < 0.05$; Fig. 7C). Subsequently, RT-qPCR analysis

was conducted to measure miR-485 expression in the tumor xenografts. The tumor xenografts derived from the miR-485 mimics group exhibited higher miR-485 expression compared with that in the miR-NC group ($P < 0.05$; Fig. 7D). Furthermore, tumor xenografts arising from the miR-485 mimics group showed decreased protein expression levels of Wnt3a, p- β -catenin and cyclin D1, as determined by western blot analysis (Fig. 7E). The total level of β -catenin protein expression was unchanged. Collectively, these results suggested that miR-485 restricted RB growth *in vivo* by directly targeting Wnt3a and regulating the Wnt/ β -catenin pathway.

Discussion

Deregulation of numerous miRNAs has been widely reported in RB, such as miR-137 (29), miR-140-5p (30), miR-448 (15) and miR-498 (31). Abnormally expressed miRNAs regulate the expression of multiple genes, and therefore may serve as critical epigenetic regulators of the occurrence and development of RB (32-34). Therefore, identification of dysregulated miRNAs in RB may provide insight into the development of effective therapeutic targets for patients with this disease. In the present study, miR-485 expression levels were detected in RB and the role of miR-485 in RB progression was investigated. Notably, the fundamental mechanisms underlying the tumor suppressor activity of miR-485 in RB cells were determined. miR-485 was expressed at low levels in RB cell lines and prohibited the malignant behavior by directly targeting Wnt3a and inhibiting activation of the Wnt/ β -catenin pathway.

miR-485 is downregulated in colorectal cancer tissues and cell lines (17,18). Low miR-485 expression is significantly correlated with tumor size, lymph node metastasis, distant metastasis and tumor-node-metastasis (TNM) stage (17). miR-485 is also decreased in gastric cancer, and its expression is closely associated with tumor size, invasion depth, lymph node metastasis and TNM stage (19). The decreased miR-485 expression levels was identified as an independent biomarker for predicting the poor clinical outcomes of patients with RB (19). Furthermore, miR-485 is expressed at low levels in glioblastoma (20,21), hepatocellular carcinoma (35,36), lung adenocarcinoma (37), breast cancer (38,39) and bladder cancer (40). However, the expression status of miR-485 in RB remains unclear. Thus, RT-qPCR was performed to determine the expression level of miR-485 in RB and it was found that miR-485 clearly demonstrated low expression in both RB tissues and cell lines. These findings suggested that miR-485 may be used as a biomarker for the diagnosis of patients with these specific malignant tumors.

miR-485 serves tumor-suppressive roles in colorectal cancer by affecting cell proliferation, apoptosis, migration and invasion (17,18). In gastric cancer, resumption of miR-485 expression prohibits cell growth and metastasis *in vitro* and inhibits tumor growth *in vivo* (41,42). In glioblastoma, ectopic expression of miR-485 prohibits cell proliferation and colony formation, impedes cell migration and invasion, induces cell apoptosis *in vitro*, and decreases tumor growth *in vivo* (20,43). miR-485 also has exhibited tumor suppressor activity in lung adenocarcinoma (37), hepatocellular carcinoma (35,36), breast cancer (38,38), bladder cancer (40), melanoma (44) and oral tongue squamous cell carcinoma (45). However, whether miR-485 contributes to the genesis and development of RB remains unclear. In the present study, the results of functional assays revealed that miR-485 overexpression restricted proliferation, promoted apoptosis and attenuated migration and invasion *in vitro* and repressed RB tumor growth *in vivo*. Therefore, miR-485 may be an attractive therapeutic target for the management of patients with these cancer types.

Multiple genes, including Growth factor receptor bound protein 2-associated binding 2 (17), cluster of differentiation 147 (18), P21 activated kinases 4 (20), stanniocalcin 2 (35), Extracellular matrix metalloproteinase inducer (36), Flotillin2 (37), Peroxisome proliferator activated receptor

γ coactivator-1 α (38), high-mobility group AT-hook 2 (40), Flotillin1 (41), nucleoside diphosphate linked moiety X-type motif 1 (42), tumor protein D54 TPD52L2 (43), Frizzled7 (44) and P21 activated kinases 1 (45) have been identified as direct targets of miR-485. Thus, the mechanisms responsible for the tumor suppressor activity of miR-485 in RB cells were explored in the present study. Wnt3a, clustered on human chromosome 1q42, was found to be a direct and functional downstream target of miR-485 in RB cells. Wnt3a was reported to be widely upregulated in numerous human malignancy types, including gastric cancer (46), colorectal cancer (47), lung cancer (48) and glioma (49). Highly expressed Wnt3a was found to contribute to the aggressive phenotype of cancers by participating in the regulation of various pathological processes, including cell growth, viability, cell cycle, apoptosis, self-renewal, metastasis, epithelial-to-mesenchymal transition, motility, differentiation and chemoresistance (26-28). In the present study, miR-485 was demonstrated to directly target Wnt3a to impede the development of RB *in vitro* and *in vivo* by regulating the Wnt/ β -catenin signaling pathway. Thus, inhibition of the Wnt3a/Wnt/ β -catenin signaling pathway using miR-485-based targeted therapy is a potential therapeutic tool for RB therapy, but this needs to be validated further.

In summary, the present data confirmed that miR-485 was remarkably downregulated in RB tissues and cell lines. Resumption of miR-485 expression suppressed the aggressive behaviors of RB cells by directly targeting Wnt3a and regulating the Wnt/ β -catenin signaling pathway, *in vitro* and *in vivo*. Understanding the specific roles of miR-485 in RB may provide further insight into the mechanisms underlying the genesis and development of RB, which may promote the development of miR-485 as a therapeutic target for treating patients with this disease. In future studies, the use of TOPFlash/FOPFlash reporter system is needed to probe for the capacity of nuclear β -catenin to bind to T cell factor/Lef transcription factors and inducing the expression of Wnt gene targets.

Acknowledgements

Not applicable.

Funding

The present study was supported by The Fund for Scientific Research Activities from China-Japan Union Hospital of Jilin University (Changchun, China).

Availability of data and materials

The data sets used and/or analyzed during the present study are available from the corresponding author upon reasonable request.

Authors' contributions

LinaW and XL designed the present study. XL and LingW performed reverse transcription-quantitative polymerase chain reactions, western blot analyses, Cell Counting Kit-8 assays and flow cytometric analysis. JL and HZ conducted the

in vitro migration and invasion assays, *in vivo* xenograft tumor formation assay, bioinformatics analyses and western blot analyses. All authors have read and approved the final draft of the manuscript.

Ethics approval and consent to participate

The present study was approved by the Ethics Committee of China-Japan Union Hospital of Jilin University (Changchun, China) and was performed in accordance with the Declaration of Helsinki and the guidelines of the Ethics Committee of China-Japan Union Hospital of Jilin University. Written informed consent was obtained from all patients for the use of their clinical tissues. All experimental procedures involving animals were approved by the Ethics Committee of China-Japan Union Hospital of Jilin University.

Patient consent for publication

Not applicable.

Competing interests

The authors declare that they have no competing interests.

References

- Dimaras H, Corson TW, Cobrinik D, White A, Zhao J, Munier FL, Abramson DH, Shields CL, Chantada GL, Njuguna F, *et al*: Retinoblastoma. *Nat Rev Dis Primers* 1: 15021, 2015.
- MacCarthy A, Draper GJ, Steliarova-Foucher E and Kingston JE: Retinoblastoma incidence and survival in European children (1978-1997). Report from the Automated Childhood Cancer Information System project. *Eur J Cancer* 42: 2092-2102, 2006.
- Houston SK, Murray TG, Wolfe SQ and Fernandes CE: Current update on retinoblastoma. *Int Ophthalmol Clin* 51: 77-91, 2011.
- Shields CL and Shields JA: Retinoblastoma management: Advances in enucleation, intravenous chemoreduction, and intra-arterial chemotherapy. *Curr Opin Ophthalmol* 21: 203-212, 2010.
- Abramson DH, Shields CL, Munier FL and Chantada GL: Treatment of retinoblastoma in 2015: Agreement and disagreement. *JAMA Ophthalmol* 133: 1341-1347, 2015.
- Mendoza PR and Grossniklaus HE: Therapeutic options for retinoblastoma. *Cancer Control* 23: 99-109, 2016.
- Kaliki S, Shields CL, Rojanaporn D, Al-Dahmash S, McLaughlin JP, Shields JA and Eagle RC Jr: High-risk retinoblastoma based on international classification of retinoblastoma: Analysis of 519 enucleated eyes. *Ophthalmology* 120: 997-1003, 2013.
- Benavente CA and Dyer MA: Genetics and epigenetics of human retinoblastoma. *Annu Rev Pathol* 10: 547-562, 2015.
- Lin S and Gregory RI: MicroRNA biogenesis pathways in cancer. *Nat Rev Cancer* 15: 321-333, 2015.
- Bracken CP, Scott HS and Goodall GJ: A network-biology perspective of microRNA function and dysfunction in cancer. *Nat Rev Genet* 17: 719-732, 2016.
- Cai Y, Yu X, Hu S and Yu J: A brief review on the mechanisms of miRNA regulation. *Genomics Proteomics Bioinformatics* 7: 147-154, 2009.
- Vasudevan S, Tong Y and Steitz JA: Switching from repression to activation: MicroRNAs can up-regulate translation. *Science* 318: 1931-1934, 2007.
- Golabchi K, Soleimani-Jelodar R, Aghadoost N, Momeni F, Moridikia A, Nahand JS, Masoudifar A, Razmjoo H and Mirzaei H: MicroRNAs in retinoblastoma: Potential diagnostic and therapeutic biomarkers. *J Cell Physiol* 233: 3016-3023, 2018.
- Wu L, Chen Z and Xing Y: MiR-506-3p inhibits cell proliferation, induces cell cycle arrest and apoptosis in retinoblastoma by directly targeting NEK6. *Cell Biol Int*: Aug 6 2018 (Epub ahead of print). doi: 10.1002/cbin.11041.
- Wu S, Ai N, Liu Q and Zhang J: MicroRNA448 inhibits the progression of retinoblastoma by directly targeting ROCK1 and regulating PI3K/AKT signalling pathway. *Oncol Rep* 39: 2402-2412, 2018.
- Liu H, Cao B, Zhao Y, Liang H and Liu X: Upregulated miR-221/222 promotes cell proliferation and invasion and is associated with invasive features in retinoblastoma. *Cancer Biomark* 22: 621-629, 2018.
- Li J, Xu J, Yan X, Jin K, Li W and Zhang R: MicroRNA-485 plays tumour-suppressive roles in colorectal cancer by directly targeting GAB2. *Oncol Rep* 40: 554-564, 2018.
- Hu XX, Xu XN, He BS, Sun HL, Xu T, Liu XX, Chen XX, Zeng KX, Wang SK and Pan YQ: microRNA-485-5p functions as a tumor suppressor in colorectal cancer cells by targeting CD147. *J Cancer* 9: 2603-2611, 2018.
- Jing LL and Mo XM: Reduced miR-485-5p expression predicts poor prognosis in patients with gastric cancer. *Eur Rev Med Pharmacol Sci* 20: 1516-1520, 2016.
- Mao K, Lei D, Zhang H and You C: MicroRNA-485 inhibits malignant biological behaviour of glioblastoma cells by directly targeting PAK4. *Int J Oncol* 51: 1521-1532, 2017.
- Wang ZQ, Zhang MY, Deng ML, Weng NQ, Wang HY and Wu SX: Low serum level of miR-485-3p predicts poor survival in patients with glioblastoma. *PLoS One* 12: e0184969, 2017.
- Livak KJ and Schmittgen TD: Analysis of relative gene expression data using real-time quantitative PCR and the 2^{-ΔΔCT} method. *Methods* 25: 402-408, 2001.
- Misiewicz-Krzeminska I, Krzeminski P, Corchete LA, Quwaider D, Rojas EA, Herrero AB and Gutiérrez NC: Factors regulating microRNA expression and function in multiple myeloma. *Noncoding RNA* 5, 2019.
- Henry JC, Azevedo-Pouly AC and Schmittgen TD: MicroRNA replacement therapy for cancer. *Pharm Res* 28: 3030-3042, 2011.
- Ors-Kumoglu G, Gulce-Iz S and Biray-Avci C: Therapeutic microRNAs in human cancer. *Cytotechnology* 71: 411-425, 2019.
- He S, Lu Y, Liu X, Huang X, Keller ET, Qian CN and Zhang J: Wnt3a: Functions and implications in cancer. *Chin J Cancer* 34: 554-562, 2015.
- Oguma J, Ozawa S, Kazuno A, Nitta M, Ninomiya Y and Kajiwarra H: Wnt3a expression is associated with poor prognosis of esophageal squamous cell carcinoma. *Oncol Lett* 15: 3100-3108, 2018.
- Qi L, Sun B, Liu Z, Cheng R, Li Y and Zhao X: Wnt3a expression is associated with epithelial-mesenchymal transition and promotes colon cancer progression. *J Exp Clin Cancer Res* 33: 107, 2014.
- Zhang J, He J and Zhang L: The down-regulation of microRNA-137 contributes to the up-regulation of retinoblastoma cell proliferation and invasion by regulating COX-2/PGE2 signaling. *Biomed Pharmacother* 106: 35-42, 2018.
- Miao X, Wang Z, Chen B, Chen Y, Wang X, Jiang L, Jiang S, Hao K and Zhang W: miR-140-5p suppresses retinoblastoma cell proliferation, migration, and invasion by targeting CEMIP and CADM3. *Cell Mol Biol* 64: 42-47, 2018.
- Yang L, Wei N, Wang L, Wang X and Liu QH: miR-498 promotes cell proliferation and inhibits cell apoptosis in retinoblastoma by directly targeting CCGP1. *Childs Nerv Syst* 34: 417-422, 2018.
- Yong-Ming H, Ai-Jun J, Xiao-Yue X, Jian-Wei L, Chen Y and Ye C: miR-449a: A potential therapeutic agent for cancer. *Anticancer Drugs* 28: 1067-1078, 2017.
- Singh U, Malik MA, Goswami S, Shukla S and Kaur J: Epigenetic regulation of human retinoblastoma. *Tumour Biol* 37: 14427-14441, 2016.
- Mirakholi M, Mahmoudi T and Heidari M: MicroRNAs horizon in retinoblastoma. *Acta Med Iran* 51: 823-829, 2013.
- Guo GX, Li QY, Ma WL, Shi ZH and Ren XQ: MicroRNA-485-5p suppresses cell proliferation and invasion in hepatocellular carcinoma by targeting stanniocalcin 2. *Int J Clin Exp Pathol* 8: 12292-12299, 2015.
- Sun X, Liu Y, Li M, Wang M and Wang Y: Involvement of miR-485-5p in hepatocellular carcinoma progression targeting EMMRIN. *Biomed Pharmacother* 72: 58-65, 2015.
- Mou X and Liu S: MiR-485 inhibits metastasis and EMT of lung adenocarcinoma by targeting Flot2. *Biochem Biophys Res Commun* 477: 521-526, 2016.
- Lou C, Xiao M, Cheng S, Lu X, Jia S, Ren Y and Li Z: MiR-485-3p and miR-485-5p suppress breast cancer cell metastasis by inhibiting PGC-1α expression. *Cell Death Dis* 7: e2159, 2016.

39. Anaya-Ruiz M, Bandala C and Perez-Santos JL: miR-485 acts as a tumor suppressor by inhibiting cell growth and migration in breast carcinoma T47D cells. *Asian Pac J Cancer Prev* 14: 3757-3760, 2013.
40. Chen Z, Li Q, Wang S and Zhang J: miR4855p inhibits bladder cancer metastasis by targeting HMGA2. *Int J Mol Med* 36: 1136-1142, 2015.
41. Kang M, Ren MP, Zhao L, Li CP and Deng MM: miR-485-5p acts as a negative regulator in gastric cancer progression by targeting flotillin-1. *Am J Transl Res* 7: 2212-2222, 2015.
42. Duan J, Zhang H, Li S, Wang X, Yang H, Jiao S and Ba Y: The role of miR-485-5p/NUDT1 axis in gastric cancer. *Cancer Cell Int* 17: 92, 2017.
43. Yu J, Wu SW and Wu WP: A tumor-suppressive microRNA, miRNA-485-5p, inhibits glioma cell proliferation and invasion by down-regulating TPD52L2. *Am J Transl Res* 9: 3336-3344, 2017.
44. Wu J, Li J, Ren J and Zhang D: MicroRNA-485-5p represses melanoma cell invasion and proliferation by suppressing Frizzled7. *Biomed Pharmacother* 90: 303-310, 2017.
45. Lin XJ, He CL, Sun T, Duan XJ, Sun Y and Xiong SJ: hsa-miR-485-5p reverses epithelial to mesenchymal transition and promotes cisplatin-induced cell death by targeting PAK1 in oral tongue squamous cell carcinoma. *Int J Mol Med* 40: 83-89, 2017.
46. Sun R, Liu Z, Tong D, Yang Y, Guo B, Wang X, Zhao L and Huang C: miR-491-5p, mediated by Foxi1, functions as a tumor suppressor by targeting Wnt3a/ β -catenin signaling in the development of gastric cancer. *Cell Death Dis* 8: e2714, 2017.
47. Lee MA, Park JH, Rhyu SY, Oh ST, Kang WK and Kim HN: Wnt3a expression is associated with MMP-9 expression in primary tumor and metastatic site in recurrent or stage IV colorectal cancer. *BMC Cancer* 14: 125, 2014.
48. Xu J, Lv W, Hu Y, Wang L, Wang Y, Cao J and Hu J: Wnt3a expression is associated with epithelial-mesenchymal transition and impacts prognosis of lung adenocarcinoma patients. *J Cancer* 8: 2523-2531, 2017.
49. Lu F, Ye Y, Zhang H, He X, Sun X, Yao C, Mao H, He X, Qian C, Wang B, *et al*: miR-497/Wnt3a/c-jun feedback loop regulates growth and epithelial-to-mesenchymal transition phenotype in glioma cells. *Int J Biol Macromol* 120: 985-991, 2018.

RETRACTED